Available online at www.sciencedirect.com
SCIENCE DIRECT®
Journal of Solid State Chemistry 177 (2004) 3903–3908
JOURNAL OF SOLID STATE CHEMISTRY
www.elsevier.com/locate/jssc

Synthesis of *Y*-type hexaferrites via a soft mechanochemical route

J. Temuujin[a], M. Aoyama[a], M. Senna[a,*], T. Masuko[b], C. Ando[b], H. Kishi[b]

[a] *Department of Applied Chemistry, Faculty of Science and Technology, Keio University, 3-14-1 Hiyoshi, Yokohama-shi, Kanagawa-ken 223-8522, Japan*

[b] *Materials Research and Development Division, General Research and Development Laboratories, Taiyo Yuden Co. Ltd, 5607-2 Nakamuroda, Gunma 370-3347, Japan*

Received 19 April 2004; received in revised form 27 May 2004; accepted 16 June 2004
Available online 18 September 2004

Abstract

Y-type ($Ba_2Co_2Fe_{12}O_{22}$) hexaferrite precursors have been prepared via a soft mechanochemical route from mixtures comprising $BaCO_3$, $Co(OH)_2$ and α-FeOOH. The mixture was activated with a multi-ring type mill for varying duration. The chemical and structural changes during grinding were examined in detail by XRD, DTA-TG, SEM, XPS and FTIR. During grinding, extended crystallinity loss or lattice disturbance was observed without an emersion of any new crystalline phases. At the same time, electronic states were changed toward the final product, fully crystallized *Y*-phase ferrite. Mechanical activation for only 1 h was sufficient to obtain a precursor for phase pure *Y*-type by subsequent heating in air at temperatures as low as 1000 °C. Development of plate-like anisotropy by using a precursor with prolonged milling was also observed. Magnetic permeability, μ', was ca. 3 at 1 GHz, equivalent to the reported data, in spite of the lower firing temperature.

Keywords: *Y*-phase hexagonal ferrite; Soft mechanochemical route; Mechanical activation; High frequency magnetic permeability

1. Introduction

Hexaferrites are very attractive materials for high frequency circuits and operating devices. They are divided into different types according to their stacking sequence, viz, *M* ($BaFe_{12}O_{19}$), *Y* ($Ba_2Me_2Fe_{12}O_{22}$), *Z* ($Ba_3Me_2Fe_{24}O_{41}$), *W* ($BaMe_2Fe_{16}O_{27}$) and *X* ($Ba_2Me_2Fe_{28}O_{46}$) types, where Me is a divalent cation from the first transition metals. From a series of hexaferrites, technical interests are gathered on *M*- and *W*-types since they are close to practical application as highly aniostropic magnetic materials.

Many techniques were applied for the synthesis of *M*-type ferrites, e.g. co-precipitation [1,2], low-temperature combustion-synthesis [3], sol–gel [4], mechanical alloying [5,6], mechanical activation [7] and solid-state synthesis [8]. In spite of its attractive magnetic properties at high frequency, *Y*-type hexaferrite has rather been regarded as an intermediate during synthesis of type *Z* ferrite. Consequently, much smaller effort was paid to synthesize phase pure *Y*-type than any other types of hexaferrite. For the synthesis of *Y*-type ferrite, conventional solid-state processes were applied [9–11] by firing at least at 1050–1100 °C. However, lower firing temperature is almost always desired to adapt industrial requirements, among others, the size and morphology control for micro devices.

A mechanochemical method, especially so-called a soft mechanochemical method has a great potential for the synthesis of inorganic precursors because of its versatility and simple operational requirements [12–14]. Soft mechanochemical reactions usually utilize surface

*Corresponding author. Tel.: +81-45-563-1569; fax: +81-45-564-0950.
E-mail address: senna@applc.keio.ac.jp (M. Senna).

0022-4596/$ - see front matter © 2004 Elsevier Inc. All rights reserved.
doi:10.1016/j.jssc.2004.06.051

hydroxyl groups, adsorbed, hydrated or contained in a hydroxide. Mechanochemical reactions then occur more beneficially as a consequence of polarization of surface hydroxyl groups. Charge transfer across the boundary of dissimilar solid species is, then, promoted, enabling formation of hetero bridging bonds between two different metallic species abridged by an oxygen atom in between. Bridging bonds in turn increase homogeneity of the reacting mixture and favor to keep the stoichiometry, being decisive for phase purity.

The objective of the present study is to examine the effects of soft mechanochemical treatment to synthesize phase pure *Y*-type hexaferrite with higher magnetic permeability at frequencies above 1 GHz by firing at lowest possible temperatures.

2. Experimental procedures

Goethite, α-FeOOH (GNA-85N), 0.2 μm long needle like morphology, with its aspect ratio 1:10, was kindly donated by Toda Kogyo Corp. Other starting materials, $BaCO_3$ (specific surface area 12.5 m^2/g and 0.2 μm long rod like morphology) and $Co(OH)_2$, were analytical grade reagents used as purchased. A stoichiometric mixture for *Y*-phase comprising $Ba(CO)_3$, α-FeOOH and $Co(OH)_2$ was activated with a multi-ring type mill, Mechano Micros® (Nara Machinery), up to 4 h. A detailed description of the mill was given elsewhere [15]. The rates of revolution and counter-revolution, respectively, of the rotor and the vessel were fixed at 1250 and 250 min^{-1}, respectively. A 30 g of the powder, corresponding to 15% of the effective volume of the vessel, was charged for each activation process. Samples were denoted as *Y–x*, where *x* represents milling time in hour. Some samples were wet ball-milled with nylon balls for 6 h and dried. It was denoted as Raw. The Raw and mechanically activated powder mixtures were calcined at 800, 950 and 1000 °C for 2 h.

Samples were characterized by a powder X-ray diffractometry (XRD, Rigaku, RINT 2000), Fourier transformed infrared spectroscopy (FTIR, Bio-Rad, Win-IR), X-ray photoelectron spectroscopy (XPS, JEOL, JPS 9000) and thermal analyses (DTA-TG, Mac Science). Particle morphology was observed by a field emission scanning electron microscope (FE-SEM, Hitachi, S-4000). Magnetic measurements were performed on the toroidal sample (7.05 mm outside diameter, 3.04 mm inside diameter and 3 mm thickness) prepared from *Y*−1, after sintering at 1200 °C for 2 h and ultrasonically machined. Density of the sintered sample was 5.029 g/cm^3, i.e. 94% of the theoretical density. Frequency dependence of the magnetic permeability was measured between 45 MHz and 6 GHz by an impedance analyzer (HP8510C, Hewlett Packard).

3. Results and discussion

3.1. Changes of crystallographical and chemical states by grinding

As shown in Fig. 1, intensity of the XRD peaks for $BaCO_3$ and α-FeOOH decreased with grinding time. However, the mixture was not fully amorphized within 4 h. Diffraction line broadening of the starting compounds was not very remarkable even after prolonged milling. This indicates that neither reduction of crystallite size nor accumulation of micro strain was significant. An exception was $Co(OH)_2$, whose diffraction peaks were almost disappeared after milling for only 1 h. This preferential degradation is ascribed to mechanochemical dehydration as referred below.

Binding energy profiles of oxygen 1s are obtained by XPS. As shown in Fig. 2, milling resulted in the oxygen 1*s* spectra for different (hydr)oxides to merge into a single broad peak similar to that of fully crystallized *Y*-phase (*Y*−1, 1000 °C) at around 530.5 eV. Ideal *Y*-phase consists of complicated block structure (T- and spinel S-blocks), where the layers are stacking along the hexagonal *c*-axis with different orientation [16]. The broad peak of crystalline *Y*-phase is attributed to the diversity of the oxygen states. From these observations, it is obvious that milling the mixture of the starting materials changes the electronic states of the different

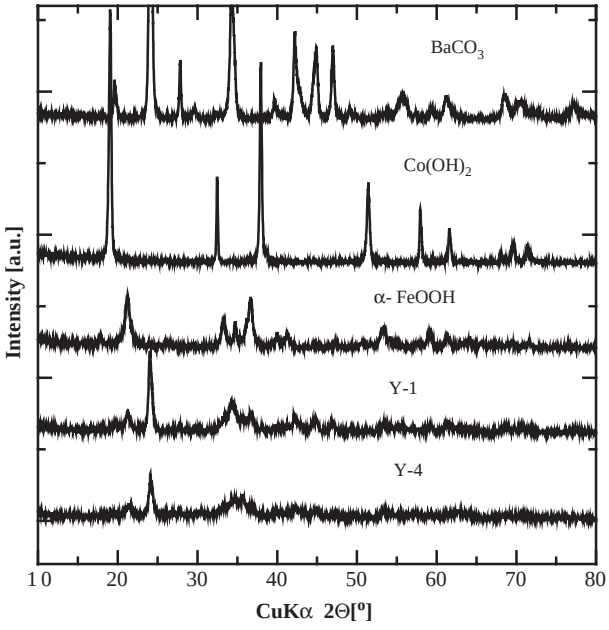

Fig. 1. XRD profiles of the starting materials and ground samples.

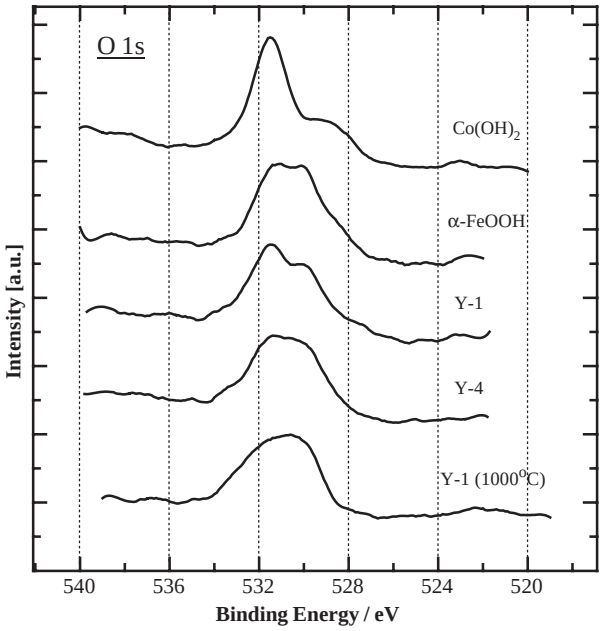

Fig. 2. XPS O1s spectra of ground and heated samples.

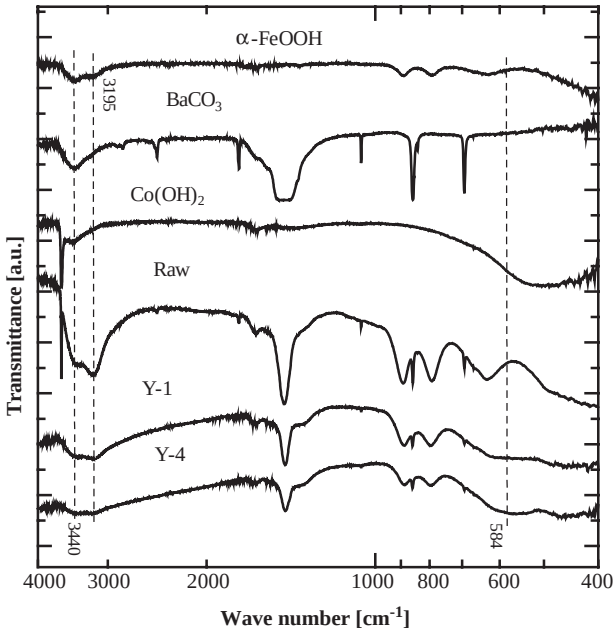

Fig. 3. FTIR spectra of the starting materials, raw and ground samples.

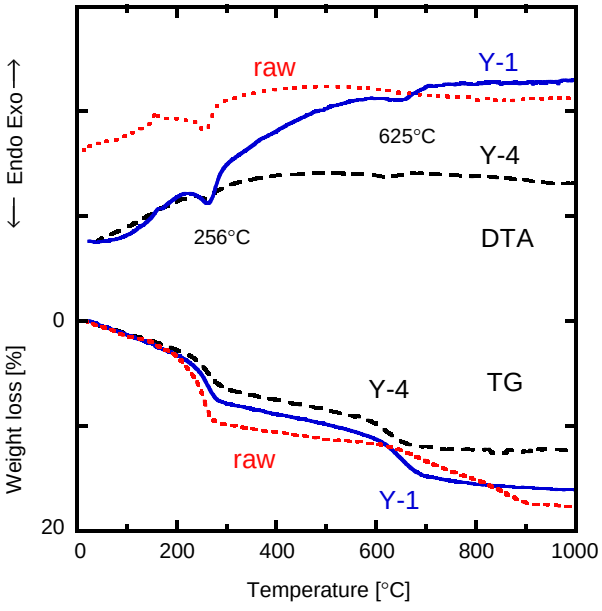

Fig. 4. TG-DTA profiles of $Y-1$ and $Y-4$ samples; heating rate 10 °C/min.

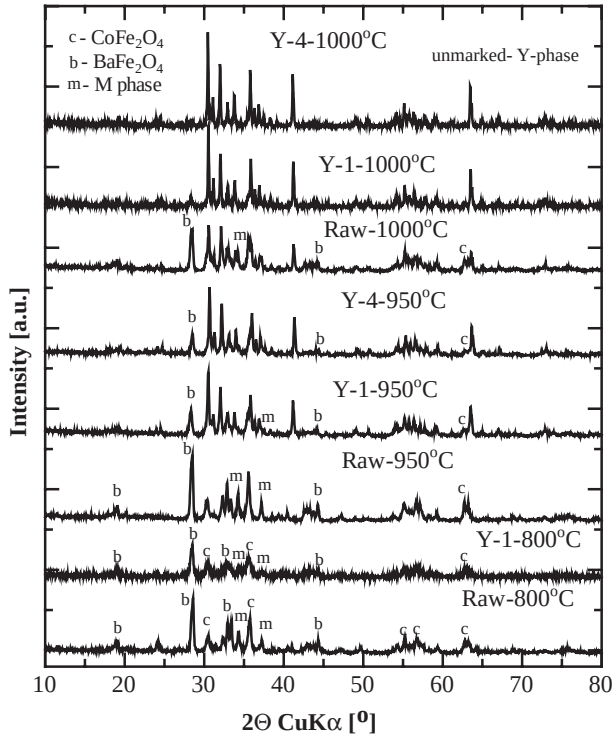

Fig. 5. XRD profiles of the Raw, $Y-1$ and $Y-4$ samples, heated under the conditions indicated.

oxygen atoms in the direction toward that of the Y-phase. These changes in XPS profile are most likely attributed to the formation of new hetero bridging bonds between different atoms, such as Fe–O–Ba or Co–O–Fe throughout the ground mixture.

OH vibration band at 3640 cm^{-1} in FTIR spectra, shown in Fig. 3, disappeared just after milling for 1 h. This accords with the disappearance of the XRD peaks of $Co(OH)_2$ mentioned above. The intensity of the absorption band at 1460 cm^{-1}, being characteristic for the carbonate groups in $BaCO_3$, also decreased by prolonged milling.

All the characteristic absorption bands of the goethite at 3195, 890, 796 and 3440 cm^{-1}, due to OH and H_2O

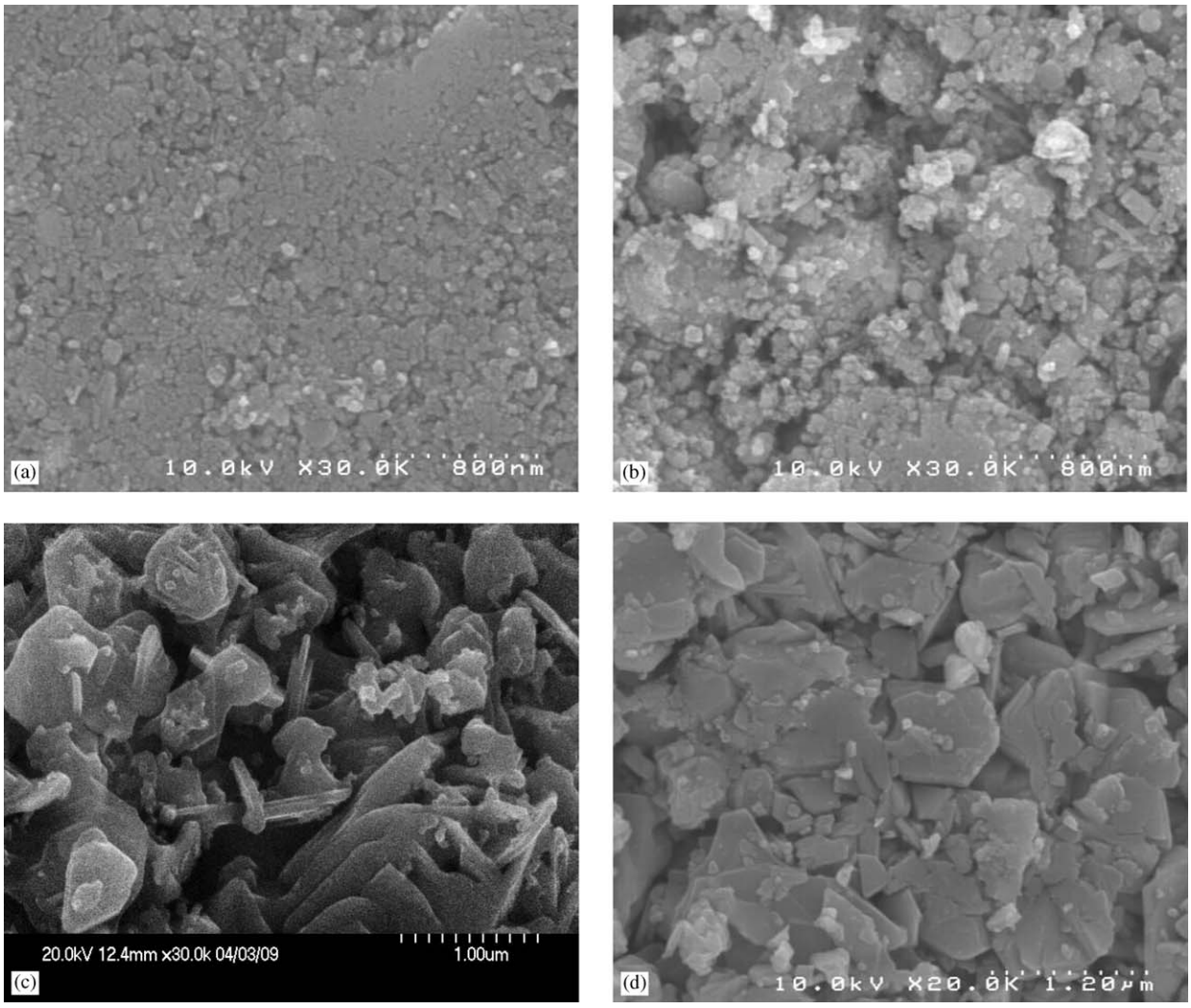

Fig. 6. FE-SEM micrographs of the ground powders (a) $Y-1$, (b) $Y-4$ and after heating at 1000 °C: (c) $Y-1$, (d) $Y-4$.

vibrations and a band at 630 cm^{-1} due to lattice vibration of the FeO_6 octahedra are quite similar with those reported previously [17]. A closer look reveals, however, that there are some changes of peak position and intensities of characteristic OH vibrations of goethite appearing at 890 and 796 cm^{-1} in $Y-1$ sample. The intensities of OH and H_2O vibrations of goethite slightly decreased in $Y-4$ sample, suggesting a partial dehydration during milling. A stretching vibration of the raw goethite, $\nu(FeO_6)$ appearing at 630 cm^{-1} became flat in $Y-1$ and broader and centered at 584 cm^{-1} for $Y-4$. We attribute these changes to substitution of Co cations into octahedral lattice of goethite and/or partial decomposition of goethite into hematite like structure [17]. The results of FTIR spectra are all in compatible with those of XPS and XRD, i.e. the change in the chemical properties of the starting mixture toward those of the target product, even prior to any heat treatment.

3.2. Thermal behavior

The DTA-TG profiles are given in Fig. 4. There are two distinct weight loss steps around 200–400 °C and 600–900 °C in the TG profile of the Raw sample, with respective endothermic peaks in the DTA curve. They are attributed to the decomposition of goethite, cobalt hydroxide and barium carbonate, respectively. The weight loss of the sample (17.4%) is higher than the theoretical loss 14.1% for reaction (1).

$$12\alpha-FeOOH + 2Co(OH)_2 + 2BaCO_3 \rightarrow 2BaO \cdot 2CoO \cdot 6Fe_2O_3 + 2CO_2 \uparrow + 8H_2O \uparrow \quad (1)$$

Weight loss (5.9%) occurring between 600 and 900 °C is slightly higher than the theoretical loss due to carbonate (5.34%). The weight loss (2.5%) occurring up to 200 °C is due to adsorbed water in the course of sample preparation because of hygroscopic nature of the starting materials.

The extent of these weight losses decreased by milling, with the lowering of the carbonate decomposition temperature. Carbonate decomposition temperature decreased due to the particle size reduction and partial amorphization, to form intimately mixed precursor. There are two clear endothermic effects in $Y-4$ at 256 and 625 °C due to dehydroxylation and decarboxylation of the residual α-FeOOH and $BaCO_3$, respectively. Total weight loss of the milled samples was also smaller than that of the Raw sample, possibly due to the evaporation of some of the surface water during grinding and mechanochemical decarboxylation. Mechanochemical dehydration and amorphous precursor formation occurs concurrently in the hydroxyl containing milling systems as a consequence of bridging bond formation [12]. We therefore suggest here again that a part of amorphized compounds is associated with the formation of hetero bridging bonds, Ba–O–Fe and Ca–O–Fe, in the precursor.

As shown in Fig. 5, $BaFe_2O_4$, $CoFe_2O_4$ and M ($BaO \cdot 6Fe_2O_3$) phases persist as intermediates after calcining the samples Raw and $Y-1$ at 800 °C. We observe little difference between $Y-1$ and $Y-4$ samples, except a slightly higher intensity of the M phase in the 4 h-milled samples (not shown). At 950 °C, considerable amount of Y-phase is observed. In samples $Y-1$ and $Y-4$, Y-phase is predominant with a small amount of spinel ($CoFe_2O_4$) and tetragonal ($BaFe_2O_4$) ferrites. Single-phase crystalline Y-phase was obtained from the precursors $Y-1$ and $Y-4$, after calcining at 1000 °C. However, when we start from Raw sample, M, $BaFe_2O_4$ and $CoFe_2O_4$ phases still coexisted. From Raw sample, phase pure Y-phase was obtained only at temperatures as high as 1150 °C. Y-phase diffraction lines are slightly stronger in $Y-4$ sample than $Y-1$. Crystallization behavior of the milled samples is in line with the previous observations on the formation of the pre-reacted precursor by X-ray photoelectron and FTIR spectra (Figs. 2 and 3). We emphasize that mechanical activation for just 1 h is enough to obtain phase pure Y-phase at temperatures as low as 1000 °C, although hetero bridging bonds are richer in $Y-4$ than in $Y-1$.

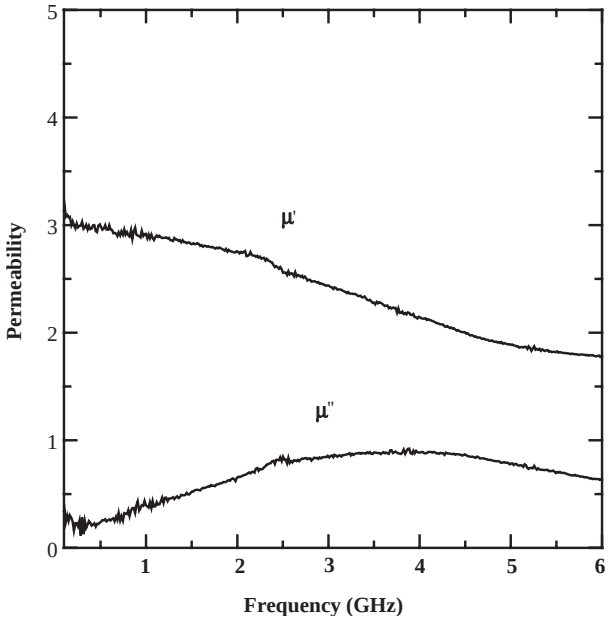

Fig. 7. Frequency dependence of the magnetic permeabilities, μ' and μ'', for sintered sample ($Y-1$).

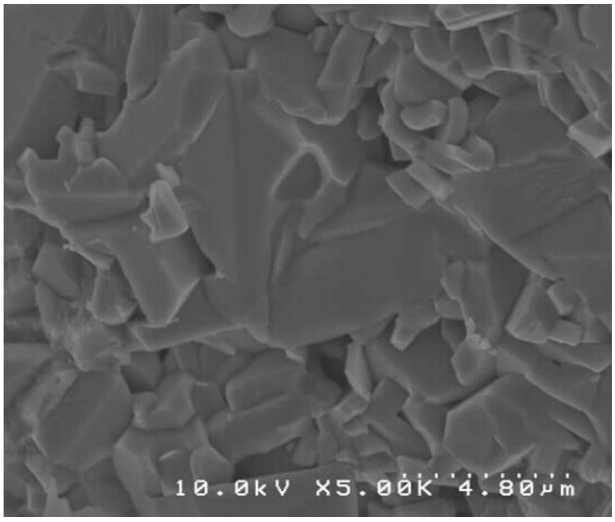

Fig. 8. Fracture surface of the Y-phase hexaferrite, sintered at 1200 °C.

3.3. Microstructure

On the micrographs shown in Fig. 6 for $Y-1$, we observe that the milled mixture comprises fine particles of about 50 nm, which reveals improved homogeneity of the starting materials. At the same time, particle morphology changes more spherical. Increasing milling time ($Y-4$) causes some agglomeration, without any other morphological change. Microstructures of $Y-1$ and $Y-4$ are similar after heating at 1000 °C. They comprise mostly plate like grains of less than 1 μm. A closer look reveals, however, that the fired sample from $Y-4$ has higher extent of anisotropy of the grains than that from $Y-1$.

3.4. Magnetic properties

Two components of magnetic permeability, μ' (real) and μ'' (imaginary), are plotted against frequency in Fig. 7. The real part, μ', remained almost constant near 3 with only a slight decrease up to 2 GHz, followed by a more rapid fall down above 2.3 GHz. The imaginary component, μ'', increased with frequency and reached a maximum at around 4 GHz. The value of the real

permeability at 1 GHz is well within the range of the reported values, 3–6 [9,10]. Microstructure, such as porosity, size and shape of the grains are known to play a significant role on the magnetic permeability. As mentioned in the experimental section, the magnetic properties were measured on the sintered sample with 94% of the theoretical density. We observe a number of pores at the grain boundary on the micrograph of the fracture surface shown in Fig. 8. They are yet to be eliminated by optimizing the sintering conditions.

4. Conclusions

Phase pure *Y*-phase hexaferrite was synthesized from the mixtures prepared by milling a hydroxyl containing mixtures of the starting compounds by a multi-ring mill for 1 h and by subsequent heating at temperatures as low as 1000 °C. This is distinctively lower than those reported in the solid state synthesis. *Y*-phase hexaferrite obtained in this work exhibits magnetic permeability equivalent to those prepared by conventional solid-state processes at higher temperatures. We therefore conclude that the soft mechanochemical method provides simple and yet technologically important processes for the preparation of *Y* type hexaferrite, particularly in favor of the synthesis at lower temperatures.

Acknowledgment

Present research was supported by COE21 program under project ''Life conjugated chemistry''.

References

[1] T. Ogasawara, M.A.S. Oliveira, J. Magn. Magn. Mater. 217 (2000) 147–154.
[2] S.R. Janasi, M. Emura, F.J.G. Landgraf, D. Rodrigues, J. Magn. Magn. Mater. 238 (2002) 168–172.
[3] J. Huang, H. Zhuang, W. Li, J. Magn. Magn. Mater. 256 (2003) 390–395.
[4] W. Zhong, W.P. Ding, N. Zhang, J.M. Hong, Q.J. Yan, Y.W. Du, J. Magn. Magn. Mater. 168 (1997) 196.
[5] J. Ding, D. Maurice, W.F. Miao, P.G. McCormick, R. Street, J. Magn. Magn. Mater. 150 (1995) 417–420.
[6] G. Mendoza-Suarez, J.A. Malutes-Aquino, J.I. Escalante-Garcia, H. Mancha-Molinar, D. Rios-Jara, K.K. Johal, J. Magn. Magn. Mater. 223 (2001) 55–62.
[7] J. Subrt, J. Tlaskal, Solid State Ionics 63–65 (1993) 110–115.
[8] H.P. Steier, J. Requena, J.S. Moya, J. Mater. Res. 14 (1999) 3647–3652.
[9] Y. Bai, J. Zhou, Z. Gui, Z. Yue, L. Li, Mater. Sci. Eng. B 99 (2003) 266–269.
[10] B. Yang, Z. Ji, G. Zhilun, L. Longtu, J. Magn. Magn. Mater. 250 (2002) 364–369.
[11] M. Obol, X. Zuo, C. Vittoria, J. Appl. Phys. 91 (2002) 7616–7618.
[12] M. Senna, Solid State Ionics 63–65 (1993) 3–8.
[13] E. Avvakumov, Chem. Sustainable Dev. 2 (1994) 475–498.
[14] J. Temuujin, Chem. Sustainable Dev. 9 (2001) 589–595.
[15] Y. Narahara, K. Hamada, M. Senna, J. Metastable Nanocryst. Mater. 15–16 (2003) 573–578.
[16] A. Colomb, J. Muller, R. Argoud., J. Magn. Magn. Mater. 130 (1994) 367–376.
[17] H.D. Ruan, R.L. Frost, J.T. Kloprogge, Spectrochim. Acta A 57 (2001) 2575–2586.